Article

Sensitivity Analysis of the Square Cup Forming Process Using PAWN and Sobol Indices

Tomás G. Parreira [1,2,*] , Diogo C. Rodrigues [1], Marta C. Oliveira [1,2] , Nataliya A. Sakharova [1,2] , Pedro A. Prates [1,2,3,4] and André F. G. Pereira [1,2]

1   Centre for Mechanical Engineering, Materials and Processes (CEMMPRE), Department of Mechanical Engineering, University of Coimbra, 3030-788 Coimbra, Portugal; marta.oliveira@dem.uc.pt (M.C.O.); nataliya.sakharova@dem.uc.pt (N.A.S.); prates@ua.pt (P.A.P.); andre.pereira@uc.pt (A.F.G.P.)
2   Advanced Production and Intelligent Systems Associated Laboratory (ARISE), 4200-465 Porto, Portugal
3   Centre for Mechanical Technology and Automation (TEMA), Department of Mechanical Engineering, University of Aveiro, 3810-193 Aveiro, Portugal
4   Intelligent Systems Associate Laboratory (LASI), 4800-058 Guimarães, Portugal
*   Correspondence: tomas.parreira@dem.uc.pt

Abstract: This study investigates the sensitivity of the square cup forming process. It analyses how the uncertainties in the material properties, friction and process conditions affect the results of the square cup, such as equivalent plastic strain, geometry change, thickness reduction, punch force and springback. The cup flange and the die curvature region are identified as highly affected areas, while the cup bottom is least affected by the uncertainties. Two sensitivity analysis techniques, PAWN and Sobol indices, are compared. In particular, the study shows that PAWN indices require a significantly smaller number of simulations than Sobol indices, making them a more efficient choice for sensitivity analysis. While both PAWN and Sobol indices generally give comparable results, discrepancies arise in the analysis of springback, where PAWN indices show superior accuracy, particularly when dealing with multimodal distributions. This observation highlights the importance of selecting the appropriate sensitivity analysis method based on the nature of the data being analysed. These results provide insights for optimizing stamping processes to reduce production time and costs.

Keywords: square cup; sensitivity analysis; PAWN indices; sobol indices

1. Introduction

Metal forming processes are widely used in automotive, aerospace, and metalworking industries due to their ability to produce complex shapes with high precision and efficiency [1]. These processes cover a wide range of techniques, including stamping, forging and extrusion, each tailored to specific applications and material properties. With the increasing demand for lightweight components with improved mechanical properties, the optimization of metal forming processes has become critical to maintaining competitiveness in the global marketplace.

Finite Element Analysis (FEA) plays a key role in predicting deformation processes and identifying factors that limit component formability. It enables the simulation of complex forming processes and the performance evaluation of different tool configurations and process parameters. However, conventional FEA approaches often overlook the inevitable uncertainties present in real-world industrial environments, a concern highlighted by several researchers [2,3]. These uncertainties arise from a variety of sources, including material variability, geometric imperfections, and process variations, and can have a significant impact on the reliability and robustness of forming simulations [4–6]. In addition, the authors in [2] pointed out that these uncertainties can change over time (e.g., due to tool wear). Ignoring these uncertainties leads to sub-optimal or unreliable forming process designs [7],

which in turn has a significant impact on component quality, scrap rates and manufacturing costs, for example due to downtime for troubleshooting and maintenance [8].

With the increasing availability of large amounts of data and improved computational capabilities, interest in stochastic modelling and quantification of uncertainties in sheet metal forming processes have been growing [9–12]. Several researchers have modelled and quantified the influence of different uncertainty sources on the final product, by resorting to distinct methods, such as Monte Carlo simulation [13,14], the design of experimental techniques [15,16] and metamodels [17,18]. In [12], an uncertainty analysis combining FEA and Monte Carlo simulation was designed to evaluate the influence of uncertainty sources on the end product. Also, in [16], the influence of the material and friction variability on the geometry of a U-channel was studied using an analysis of variance (ANOVA), with them reaching the conclusion that the parameters C and n of the Swift hardening law were the most influential factors in the springback and maximum thinning results. In another piece of research, [18], a metamodel was used based on machine learning techniques to predict the occurrence of defects, considering the variability in the material properties and process parameters. In [17], the authors compared the performance of various metamodel techniques by considering the uncertainties in the material behaviour and sheet thickness. The authors concluded that some metamodel techniques are able to accurately predict the forming process results. The application of any of the presented methods requires the execution of several numerical simulations of the forming process. To reduce the computational cost of these strategies, screening techniques can be used to select the main sources of uncertainty to be considered in the stochastic model [16].

A sensitivity analysis is traditionally performed using analysis of variance (factorial ANOVA). However, this approach assumes a unimodal distribution of results, which is not necessarily true. Factorial ANOVA also requires a model to be predefined to establish a correlation between the factors and the results [16]. Sobol indices (also referred to as functional ANOVA [19]) can address this problem by not requiring a hypothesis in the form of a model, but have the limitation of only being reliable for unimodal data. The PAWN indices appear as a technique that can overcome both of these vulnerabilities [20,21], as they do not rely on a statistical second-order moment (i.e., variance) [22]. Instead, PAWN indices use the Cumulative Distribution Functions to evaluate the influence of the different factors on the results.

Although PAWN sensitivity analysis can present a promising alternative to the above-mentioned approaches, its application in the sheet metal forming process is still unexplored. The goal of this work is to explore the use of PAWN sensitivity analysis, by investigating the sensitivity of the square cup forming process to material properties, friction, and process conditions. The results of the PAWN indices will be compared to the Sobol indices, obtained in a previous sensitivity analysis [23]. By employing sensitivity analysis techniques such as PAWN and Sobol indices, the aim is to identify key parameters influencing the forming process of a square cup and provide insights for optimizing process parameters to mitigate the effects of uncertainties.

2. Numerical Model

A schematic representation of the square cup forming process is shown in Figure 1, with tool geometries based on the benchmark proposed by the NUMISHEET' 93 conference [24]. Throughout the process, a constant blank holder force (BHF) is used to control the material flow. The punch is then advanced to a total displacement of 40 mm. At the end, the square cup is extracted from the tools, promoting the springback of the square cup. To optimize the computational efficiency, only a quarter of the model is simulated, taking advantage of material and geometric symmetries. The square blank, with an initial thickness of t_0 and a side length of 75 mm, is discretized into 1800 elements using 8-node hexahedral solids, with 2 elements in thickness and 30 elements per side. This mesh guarantees an error inferior to 1% in the maximum yield stress and a simulation time inferior to 5 min (as can be concluded from Figure 1c). The interaction between the blank and the tools is governed by

Coulomb's law, using a constant coefficient of friction μ_0. The contact with friction problem is solved using the augmented Lagrangian method. The tools are rigid, represented using Nagata patches [25], and are only allowed to displace on the vertical direction, being the displacement of the blank holder controlled by the imposed force (*BHF*). Computational simulations were performed using the in-house code DD3IMP (Deep Drawing 3D Implicit Code) [26], which uses an updated Lagrangian scheme to integrate the constitutive law in an implicit way. All numerical simulations were performed on computers equipped with an Intel® Core™ i7-8700K Hexa-Core processor 4.7 GHz. On average, each simulation took approximately 4 min and 34 s to complete.
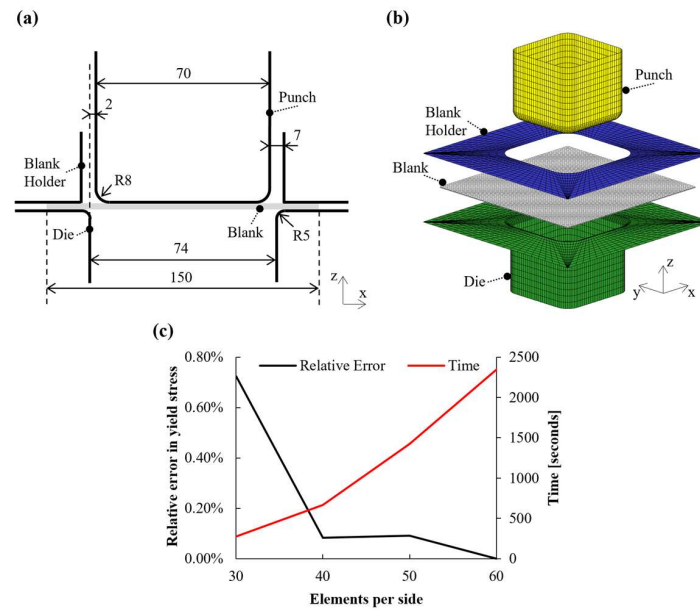
Figure 1. Square cup forming process: (**a**) dimensions of the tools in mm; (**b**) numerical model. adapted with permission from [18]; (**c**) mesh sensitivity.

A low-carbon steel (DC06) was considered as the material of the sheet. The plastic behaviour is described by the Hill'48 orthotropic yield criterion [27] and the Swift work hardening law [28]. The Hill'48 orthotropic yield criterion is defined as follows:

$$F(\sigma_{yy} - \sigma_{zz})^2 + G(\sigma_{zz} - \sigma_{xx})^2 + H(\sigma_{xx} - \sigma_{yy})^2 + 2L\tau_{yz}^2 + 2M\tau_{xz}^2 + 2N\tau_{xy}^2 = Y^2, \quad (1)$$

where Y is the yield stress; F, G, H, L, M and N are the parameters that define the shape of the yield surface; and σ_{xx}, σ_{yy}, σ_{zz}, τ_{xy}, τ_{xz} and τ_{yz} are components of the Cauchy stress tensor, written in the orthotropic coordinate system 0_{xyz}. In this work, it is assumed that $L = M = 1.5$ (identical to von Mises) and the condition $G + H = 1$, meaning that the yield stress, Y, is comparable to the uniaxial tensile stress aligned with the rolling direction.

The anisotropy coefficients for $0°$, $45°$ and $90°$ (relative to the rolling direction), respectively denoted by r_0, r_{45} and r_{90}, can be determined by following the equations:

$$r_0 = \frac{H}{G}, \quad (2)$$

$$r_{45} = \frac{N}{F + G} - \frac{1}{2}, \quad (3)$$

$$r_{90} = \frac{H}{F}, \quad (4)$$

The yield stress (Y) evolution with plastic deformation is described by the Swift hardening law:

$$Y = C\left(\varepsilon_0 + \bar{\varepsilon}^p\right)^n, \quad (5)$$

where C, ε_0 and n are material constants, and $\bar{\varepsilon}^p$ represents the equivalent plastic strain derived from the Hill'48 orthotropic yield criterion by assuming an associated flow rule. The initial yield stress, Y_0, is given by:

$$Y_0 = C\varepsilon_0^n. \tag{6}$$

This study will focus on investigating the influence of the uncertainty in the material properties, friction and the forming process conditions on the stamping of the square cup. Therefore, the input parameters of the numerical model whose influence will be studied are Young's modulus (E), Poisson's ratio (ν), anisotropy coefficients (r_0, r_{45} and r_{90},), the initial yield strength (Y_0), the hardening coefficient (n), the parameter C of the Swift law, the initial sheet thickness (t_0), the coefficient of friction (μ_0) and the blank holder force (BHF). The uncertainty in the input parameters, associated with the material properties, friction, and process conditions, is assumed to follow a normal distribution with a given mean (μ) and standard deviation (σ), as shown in Table 1. The mean values of the constitutive parameters, blank thickness and friction coefficient were obtained from [16] based on the NUMISHEET' 93 Benchmark. The mean value of the blank holder force was optimized in a previous work [17]. The standard deviations were obtained from [16] based on a literature review, except the Poisson ratio, friction coefficient and blank holder force that were based on empirical assumptions made in [17].

Table 1. Input's mean and standard deviation, reprinted with permission from [16] AIP publishing 2018 and [17].

	E [GPa]	ν	r_0	r_{45}	r_{90}	Y_0 [MPa]	n	C [MPa]	t_0 [mm]	μ_0	BHF [N]
μ	206.00	0.300	1.790	1.510	2.270	157.12	0.259	565.32	0.780	0.1440	9800.0
σ	3.85	0.015	0.051	0.037	0.121	7.16	0.018	26.85	0.013	0.0288	490

The influence of the uncertainty in these input parameters was studied on the numerical results of the square cup, i.e., the output parameters of the model: punch force (PF), equivalent plastic strain (EPS), thickness reduction (TR), geometry changes (GC) and springback (SB). The PF and the EPS values are directly obtained from the numerical simulation, while the TR, the GC and SB are defined by:

$$\text{TR } [\%] = 100 \times \left(t_0 - t_f\right)/t_0, \tag{7}$$

$$\text{GC } [mm] = \sqrt{\left(\bar{x}_f - x_f\right)^2 + \left(\bar{y}_f - y_f\right)^2 + \left(\bar{z}_f - z_f\right)^2}, \tag{8}$$

$$\text{SB } [mm] = \sqrt{\left(x_f - x_{bs}\right)^2 + \left(y_f - y_{bs}\right)^2 + \left(z_f - z_{bs}\right)^2}, \tag{9}$$

where t_0 and t_f are the initial and final sheet thickness, respectively, evaluated for each node of the square cup numerical model; (x_f, y_f, z_f) and $(\bar{x}_f, \bar{y}_f, \bar{z}_f)$ are, respectively, the final spatial position of a given node for the numerical simulation with and without uncertainty (i.e., using the mean values of Table 1); and (x_{bs}, y_{bs}, z_{bs}) is the spatial position of a given node before the springback, i.e., before removing the tools. The GC quantifies the positional difference of a given node between the deterministic and the stochastic simulation, i.e., it is a measure of the shape accuracy between the desired cup shape and the final shape that is affected by the uncertainty. The SB quantifies the positional difference of a given node before and after removing the tools, i.e., it is a measure of the springback.

The variability in the forming results was evaluated using a quasi-Monte Carlo method coupled with Sobol sequence to generate the sample of input parameters according to the normal distributions given in Table 1. A sample size of 3000 simulations of the square cup was chosen to ensure the convergence of the statistical measures, mean and standard deviation. Figure 2 shows the mean and standard deviation for the results of EPS, TR,

GC and SB along the square cup [23]. From this figure, it can be seen that the equivalent plastic strain reached its maximum at the wall and side edges of the flange, with the most pronounced dispersion of its values occurring in the latter region. In the case of thickness reduction, the highest mean values occurred at the cup wall, with significant standard deviation values only at the flange edge. The mean and standard deviation value for the geometry changes were higher at the flange edge and wall. The highest mean and standard deviation values for the springback occurred at the flange edge. The bottom of the cup is the only area where the uncertainty of the input parameters did not affect the cup results, making a sensitivity analysis in this area unnecessary. Figure 3 shows the evolution of the mean and standard deviation of the force applied by the punch as a function of its displacement. The force reaches maximum values between 17 and 30 mm of displacement and the standard deviation was higher within this range of values, indicating that it is during this phase of displacement that the uncertainty of the input parameters has the greatest effect on the force variability of the punch.
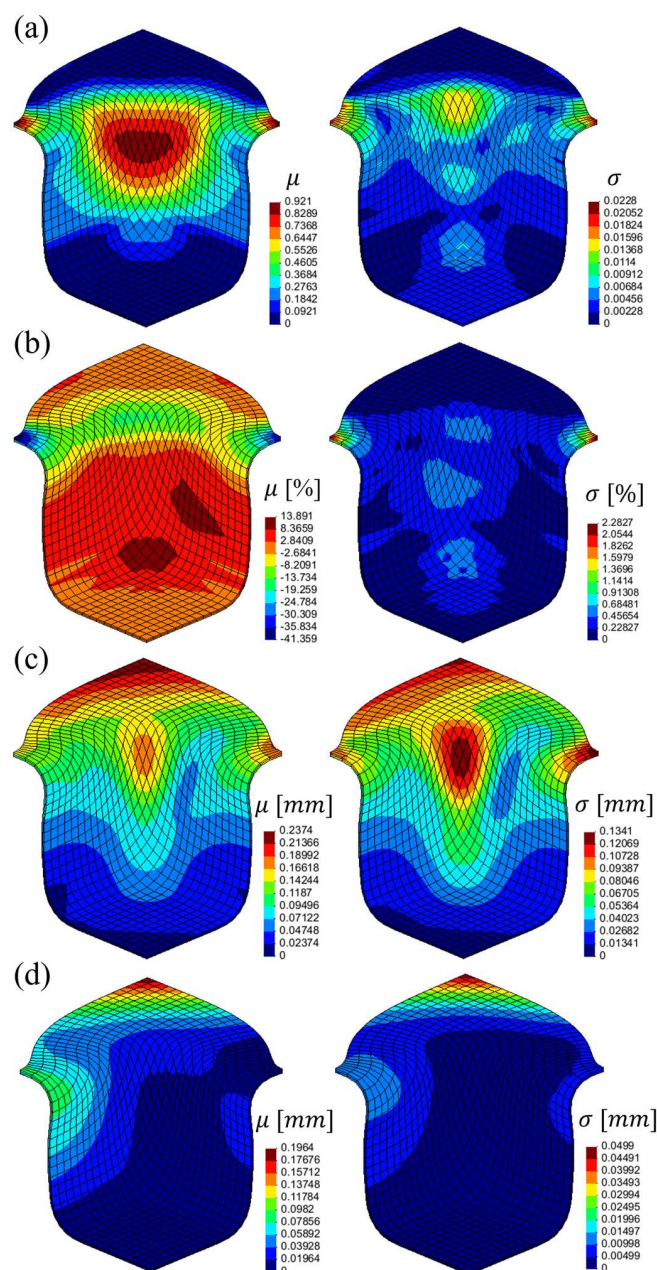

Figure 2. Plots of mean and standard deviation for (**a**) EPS, (**b**) TR, (**c**) GC, (**d**) SB.
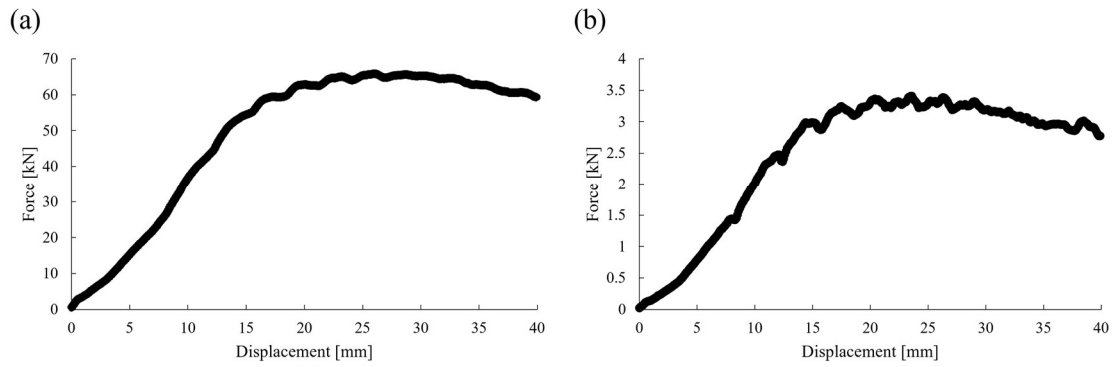
Figure 3. Evolution of the mean (**a**) and standard deviation (**b**) of the force applied by the punch.

Figure 4 shows the distributions of the maximum values of each output parameter (i.e., forming results). All outputs follow central tendency distributions, except for the springback (Figure 4e). It is important to consider the distributions of each output variable because, as noted above, the distributions of the results limit the sensitivity analysis that can be applied. In particular, the distribution associated with springback (Figure 4e) is an obstacle to the use of variance-based approaches (e.g., Sobol indices and factorial ANOVA), as these are not appropriate for data that do not follow a distribution with central tendency.
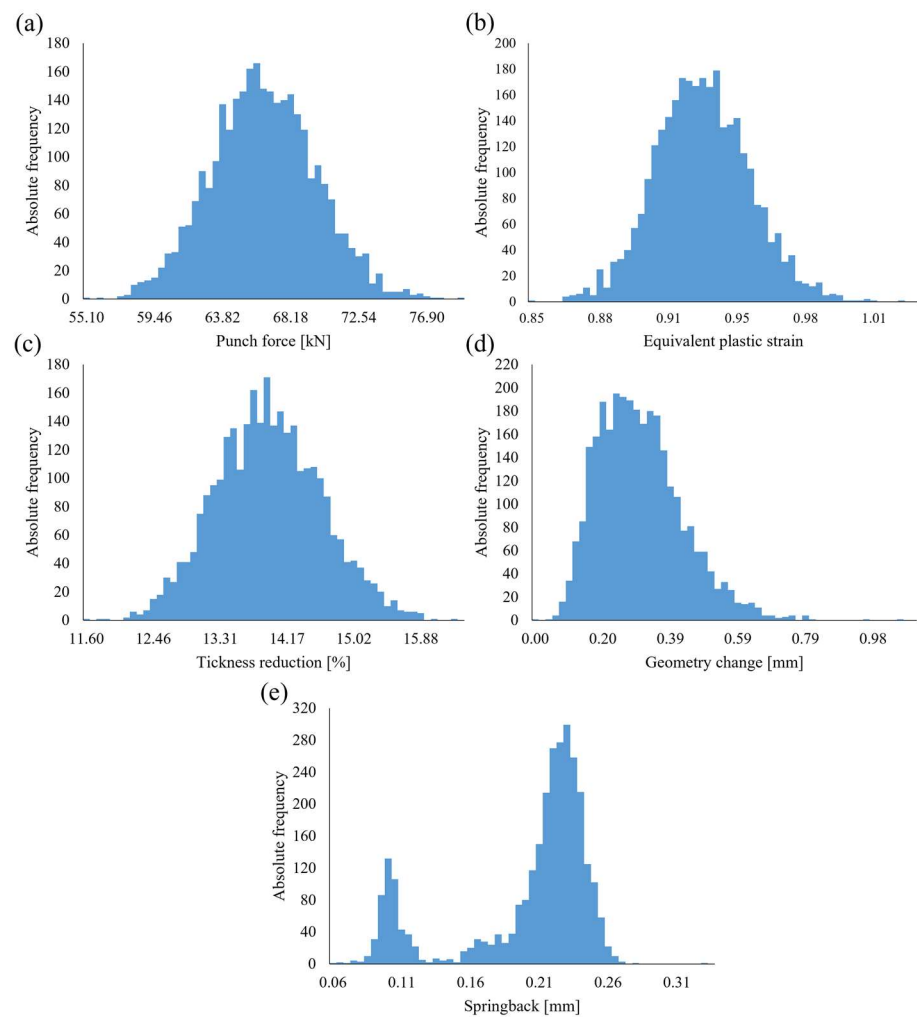
Figure 4. Distribution of maximum model response for (**a**) PF; (**b**) EPS; (**c**) TR; (**d**) GC; and (**e**) SB.

3. Sensitivity Analysis

The PAWN indices are a sensitivity analysis technique based on the cumulative distribution function of a given data sample, as opposed to other techniques (Sobol and factorial ANOVA) based on the variance of the probability density functions [20]. This allows PAWN indices to be applied to samples that follow more complex distributions, i.e., multimodal distributions. The basic concept behind these indices is that the influence of an input is related to the change produced in the cumulative distribution function of an output.

The first approach proposed for deriving PAWN indices, for a given output y, is to compare cumulative distribution functions [20]. Specifically, the cumulative distribution function obtained by assuming that all input parameters vary, $\widehat{F}_y(y)$, is compared with other n functions, $\widehat{F}_{y|x_i}(y)$, obtained by assuming a fixed value for a particular input parameter, x_i, while varying the remaining input parameters. The n functions $\widehat{F}_{y|x_i}(y)$ are derived for different fixed values of x_i. The PAWN index, P_i, for the parameter x_i was obtained through a statistical measure, such as the average of the Kolmogorov–Smirnov statistics between the function $\widehat{F}_y(y)$ and the n functions $\widehat{F}_{y|x_i}(y)$ with the input parameter x_i fixed. The PAWN index, P_i, is defined by the following equation:

$$P_i = mean_{x_i = \overline{x_i}^{(1)}, \ \overline{x_i}^{(2)}, \dots, \overline{x_i}^{(n)}} \left(\widehat{KS}(x_i) \right), \tag{10}$$

where $\widehat{KS}(x_i)$ is the Kolmogorov–Smirnov statistic that quantifies the difference between the cumulative distribution functions $\widehat{F}_y(y)$ and one of the n cumulative distribution functions $\widehat{F}_{y|x_i}(y)$ when the input parameter x_i is fixed at a given value $\overline{x_i}^{(n)}$. The statistic $\widehat{KS}(x_i)$ is obtained by the following expression:

$$\widehat{KS}(x_i) = \left| \widehat{F}_y(y) - \widehat{F}_{y|x_i}(y) \right|, \tag{11}$$

Subsequently, a more efficient approach [21] was proposed that allows the use of generic sampling (i.e., it is not mandatory to assume fixed values for the input parameter x_i). The new approach allows PAWN indices to be calculated, starting by dividing the input parameter domain x_i into n equal intervals and obtaining the cumulative distribution functions for each of the n subdomains, $\widehat{F}_{y|x_i}(y)$. In addition, the cumulative distribution, $\widehat{F}_y(y)$, was calculated for the entire data set, i.e., the entire domain of x_i. Similarly to the first approach, the maximum vertical difference was calculated (using the Kolmogorov–Smirnov statistic) between the cumulative distribution curve of each data interval, $\widehat{F}_{y|x_i}(y)$, and the cumulative distribution curve of the entire data set, $\widehat{F}_y(y)$. The value of the PAWN index, P_i, for the parameter x_i was calculated using Equation (9).

The Sobol indices are a sensitivity analysis technique based on the calculation of the variance (i.e., based on the probability distribution function), unlike the PAWN indices which are based on the calculation of the cumulative distribution function. The variance is a parameter of central tendency that represents the average of the squares of the difference between the value of the mean of a given distribution and the value of each of its constituent points. The Sobol Indices (total sensitivity indices) were calculated using the following equation [29]:

$$S_i^T = 1 - \frac{V[E(y|x_{\sim i})]}{V(y)}, \tag{12}$$

where $V(y)$ is the unconditional variance of the output parameter y and $V[E(y|x_{\sim i})]$ is the conditional variance of the expected value of the output parameter y when varying all the input parameters except $x_{\sim i}$.

The fact that Sobol indices are based on variance means that they only have accurate results for unimodal distributions. Bearing this in mind, it is expected that the results obtained by the PAWN indices for the springback output parameter will be different from the results obtained by the Sobol indices for the same parameter. On the other hand, PAWN indices have the disadvantage of requiring the calculation of cumulative

distribution functions, whereas Sobol indices only require the calculation of variance. Another disadvantage of PAWN indices is that it is necessary to define the number of intervals into which the data are divided, which is another factor that can influence the results. Both indices quantify the influence of the parameter uncertainty on the forming results in the same way; i.e., the higher their values are, the higher is the influence of a given input uncertainty on the result variability. For indices close to zero there is no influence on the result.

3.1. Stabilization Analysis

The indices are considered to be stabilized when their variation is equal to or less than 5%. This stabilization criterion is the same for all input parameters and is validated for successive intervals of 500 simulations, i.e., for 500, 1000, 1500, 2000, 2500 and 3000 simulations. The stabilization analysis of the indices was calculated considering the maximum values of the output parameters. From Figure 5, in the case of punch force, equivalent plastic strain and thickness reduction, the value of the PAWN and Sobol indices stabilized with the use of 2500 and 1500 base simulations, respectively. For the geometry change, the PAWN and Sobol indices stabilized their value when more than 2000 simulations were used. For the springback, the PAWN and Sobol indices stabilized when more than 1500 simulations were used. It is worth noting that in the case of the Sobol indices, a base sample of m simulations requires a total of $m \times (11+2)$ simulations to evaluate the sensitivity indices for the 11 input parameters, according to the traditional procedure [30]. It is therefore evident that the computation of the PAWN indices is clearly more efficient.

Figure 6 shows the results of the PAWN and Sobol indices for the maximum values of the output parameters. The figure shows that the uncertainty in the C parameter of Swift's law has the greatest influence on the variability of the punch force (Figure 6a). The variability in the equivalent plastic strain is most influenced by the uncertainty in the hardening coefficient n, and in the anisotropy coefficient, r_{90} (Figure 6b). The variability in the thickness reduction is most affected by the hardening coefficient n, and the anisotropy coefficient, r_{90} (Figure 6c). As for the variability in the geometry changes (Figure 6d), the anisotropy coefficients r_{90} and r_0 are the ones that have greater importance for the PAWN indices. For the Sobol indices, r_{90} and r_{45} are the most important inputs. In the springback (Figure 6e), the results are similar in terms of which parameters are more influential, although there is a significant discrepancy in the values of the indices. The most influential parameters in this case are the hardening coefficient n, the parameter C and the blank holder force. The uncertainties that most influence the variability in the punch force, equivalent plastic strain and thickness reduction, are similar for the PAWN and Sobol indices. However, for the geometry change and springback, the most influential uncertainties are different for the PAWN and Sobol indices.

3.2. Pareto Analysis

In this section, a Pareto analysis is performed on the results of the indices to separate the more important from the less important input parameters. Figures 7 and 8 show the graphs corresponding to the Pareto analysis for both sensitivity analysis techniques, where the vertical bars represent the absolute value of the index for the parameter in question and the black curve represents the accumulated percentage. According to Pareto, the most important parameters are those that contribute to 80% of the variability of the output parameters. From Figures 7 and 8, it can be observed that the results of the Sobol indices consider that a small number of uncertainty factors (at most six input parameters) are responsible for 80% of the output variability. On the other hand, the PAWN indices consider that a large number of uncertainty factors (at least six input parameters) are responsible for 80% of the output variability.
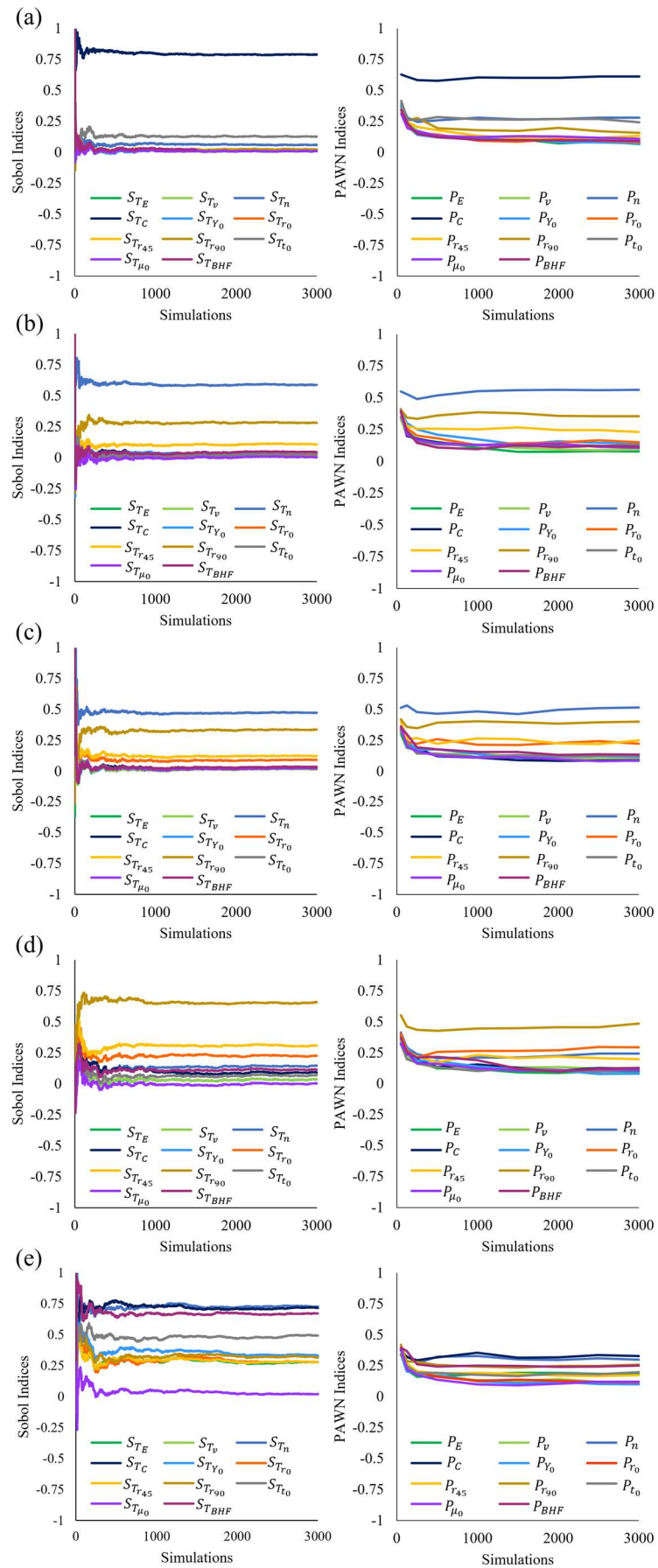
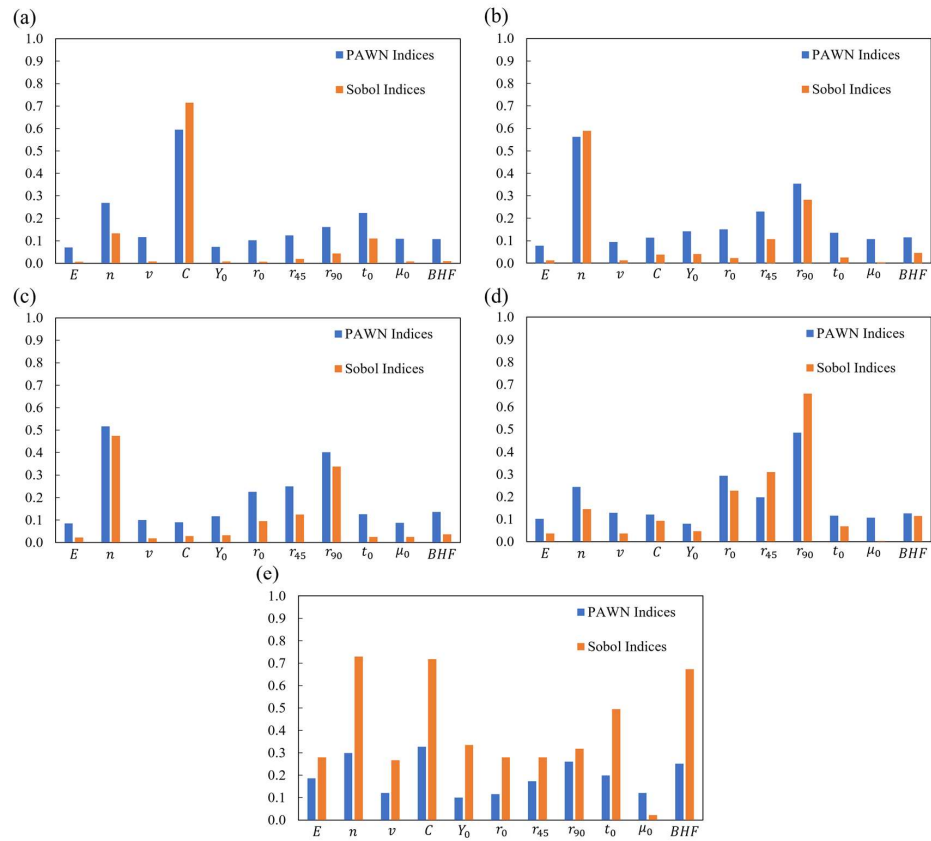**Figure 5.** Stabilization analysis for (**a**) PF; (**b**) EPS; (**c**) TR; (**d**) GC; and (**e**) SB.

Figure 6. Sobol and PAWN indices for (**a**) PF; (**b**) EPS; (**c**) TR; (**d**) GC; and (**e**) SB.
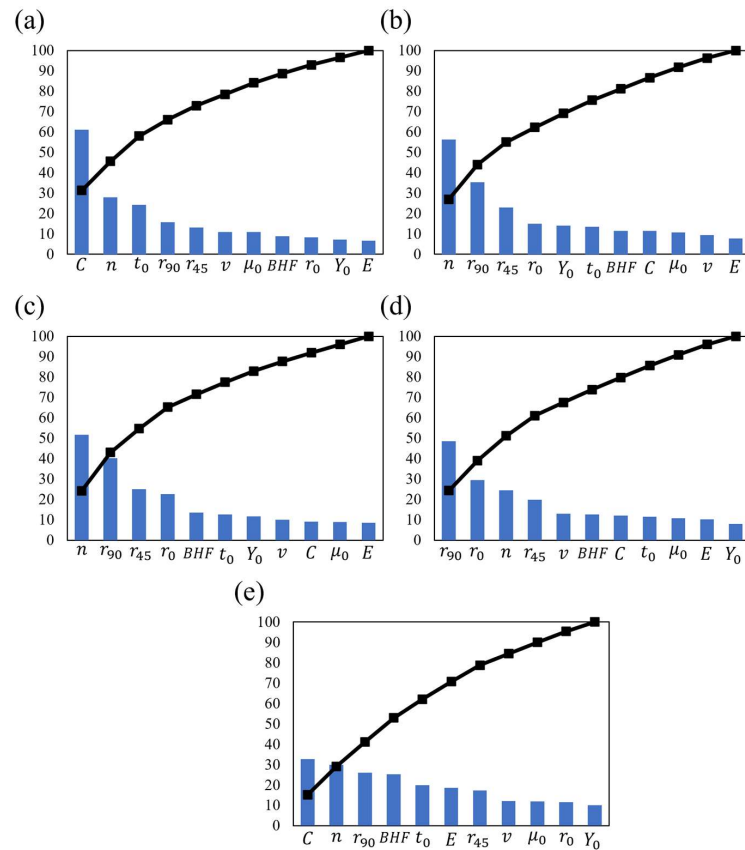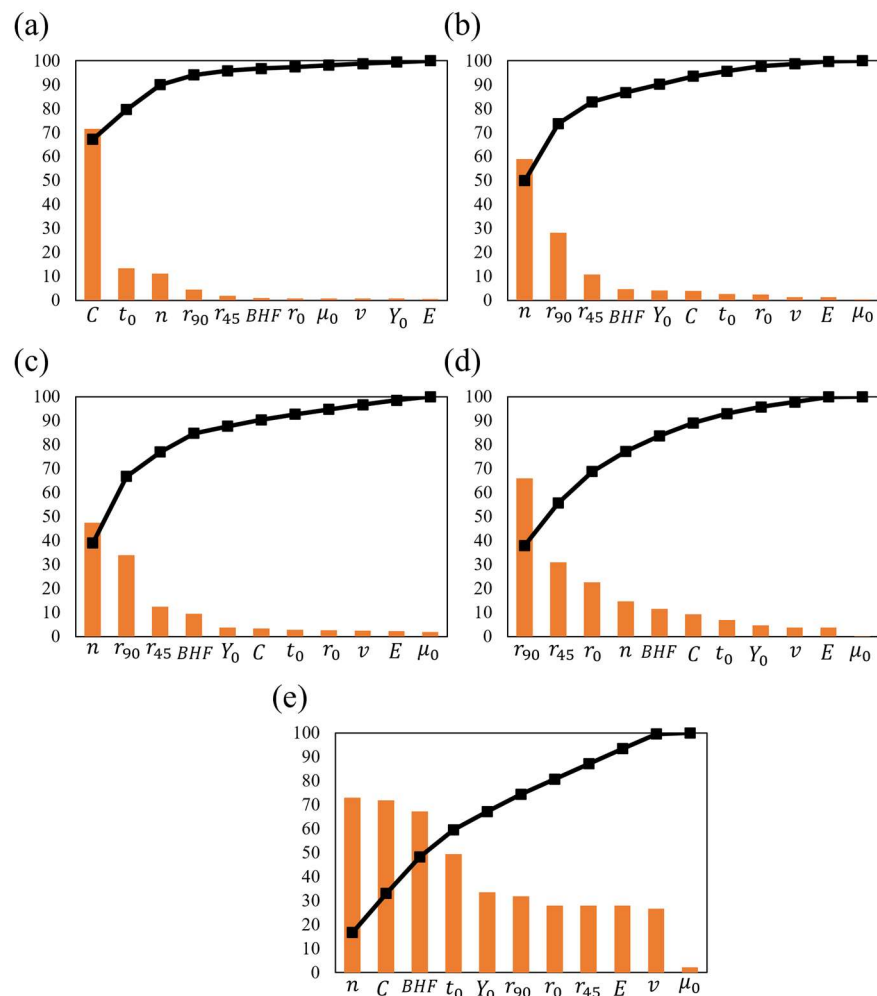

Figure 7. Pareto analysis for PAWN indices for the responses (**a**) PF; (**b**) EPS; (**c**) TR; (**d**) GC; and (**e**) SB.

Figure 8. Pareto analysis for Sobol indices for the responses (**a**) PF; (**b**) EPS; (**c**) TR; (**d**) GC; and (**e**) SB.

From Figures 7 and 8, it can be concluded that for the punch force, according to the Sobol indices, 80% of the variability is associated with the uncertainties in the C parameter of Swift's law and the initial thickness (Figure 8a). In addition to these parameters, the PAWN indices also identify the uncertainties in the hardening coefficient, the anisotropy coefficients at 45° and 90°, and the Poisson ratio as being responsible. As for the equivalent plastic strain, the Sobol indices (Figure 8b), 80% of the variability comes from the uncertainties in the hardening coefficient and the anisotropy coefficient at 90°. In addition to these parameters, the PAWN indices (Figure 7b) show that 80% of the variability in the equivalent plastic strain is caused by the uncertainty in the anisotropy coefficients at 0° and 45°, the initial yield stress and the initial blank thickness.

The variability in the thickness reduction is significantly affected by the uncertainty in the hardening coefficient, the anisotropy coefficients at 0°, 45° and 90°, the BHF and the initial thickness, according to the PAWN indices (Figure 7c). For the Sobol indices (Figure 8c), only the uncertainties of the hardening coefficient and the anisotropy coefficients at 45° and 90° account for 80% of the thickness reduction variability. For the PAWN indices, the variability in the geometry changes is due to the uncertainties in the anisotropy coefficients at 0°, 45° and 90° and the hardening coefficient, the Poisson ratio and the BHF (Figure 7d). In the case of the Sobol indices (Figure 8d), the uncertainty in the anisotropy coefficients and the hardening coefficient are the most important. For the springback, both indices (Figures 7e and 8e) assume that 80% of the variability is due to the uncertainty in the parameter C of Swift's law, the BHF, the hardening coefficient, the anisotropy coefficients at 90°, and the Young's modulus (for PAWN indices) or the initial yield stress (for Sobol

indices). In summary, the main uncertainty factors are similar for both sensitivity analyses, although the PAWN sensitivity shows that the results are influenced by more factors.

3.3. Sensitivity Indices per Region of the Square Cup

Sensitivity indices are calculated for the different regions of the square cup. The aim of this analysis is to understand, for the different output parameters, which uncertainties in the input parameters are most influential in different regions of the cup. For the equivalent plastic strain, the uncertainty in the hardening coefficient (Figure 9a) has a significant influence in the central region of the wall and at the radius of curvature of the punch. Since the maximum variability of the equivalent plastic strain is observed in the central region of the wall (see Figure 2a), it is therefore essential to control the uncertainty in the hardening coefficient. The uncertainty in the anisotropy coefficient at 90° significantly influences the equivalent plastic strain variability in the radius of curvature of the die and in the upper region of the cup wall, which is also a critical region with a high variability in the equivalent plastic strain values (see Figure 2a). The results obtained are qualitatively similar for both indices.
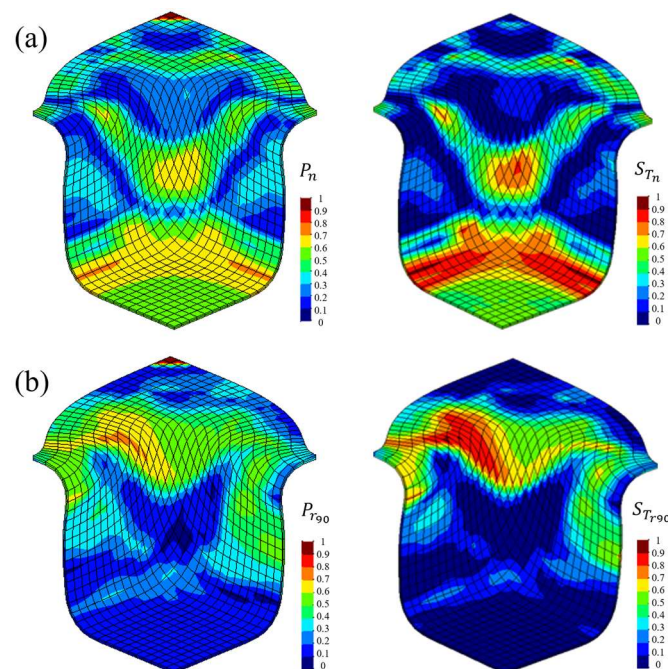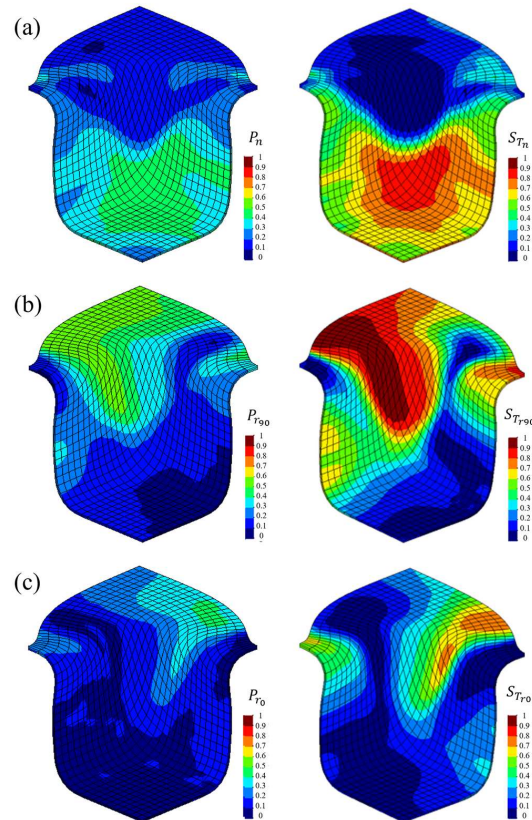

Figure 9. Distribution of PAWN (**left**) and Sobol (**right**) indices for equivalent plastic strain: (**a**) n; (**b**) r_{90}.

From Figure 10, it can be concluded that the variability in the thickness reduction, at the bottom of the cup, along the radius of curvature of the punch and in the central region of the wall (Figure 10a) is significantly influenced by the uncertainty in the strain hardening coefficient. Although the variability at the bottom of the cup is not significant (see Figure 2b), along the radius of curvature of the punch and in the central region of the wall there is a significant variability in the thickness reduction (see Figure 2b), so the uncertainty in the hardening coefficient is essential to control. The uncertainty in the anisotropy coefficient at 90° (Figure 10b) significantly affects the variability of the thickness reduction in the cup wall, the radius of curvature of the die and the flange. However, only the wall zone has a significant variability in thickness reduction (see Figure 2b), which means that the uncertainty of the anisotropy coefficient at 90° is particularly critical in this region. The results obtained are qualitatively similar for both indices.
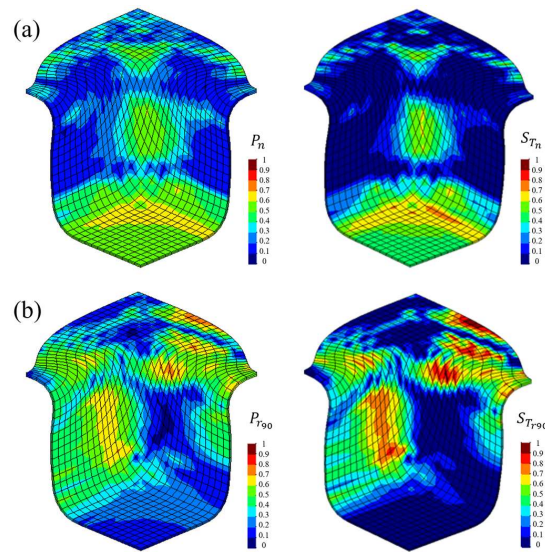
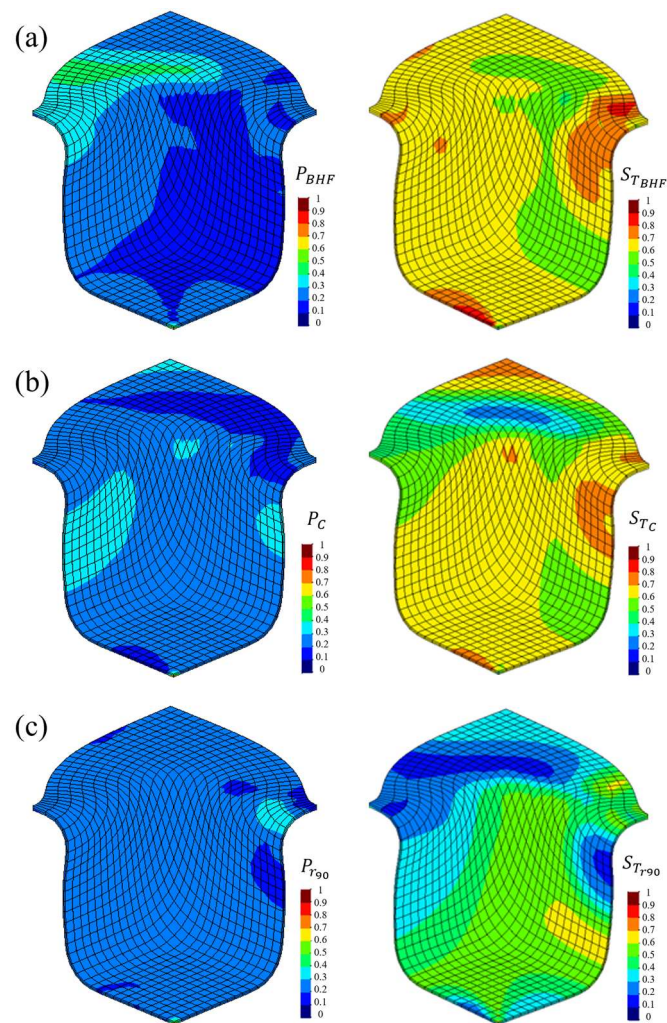**Figure 10.** Distribution of PAWN (**left**) and Sobol (**right**) indices for thickness reduction: (**a**) n; (**b**) r_{90}.

Figure 11a shows that the variability in the geometry changes is influenced by the hardening coefficient at the bottom of the wall and at the bottom of the cup. The uncertainty in the anisotropy coefficients at 0° and 90° (Figure 11b,c) largely influence the variability of the geometry changes in the upper part of the square cup. These areas coincide with the regions of the cup where the variability in the geometry change is significant (see Figure 2c). Therefore, to control the variability of the geometry change, it is more important to control the uncertainty in the anisotropy coefficients at 0° and 90° than in the hardening coefficient. The results obtained were qualitatively similar for both indices.

Figure 11. Distribution of PAWN (**left**) and Sobol (**right**) indices for the geometry changes: (**a**) n; (**b**) r_{90}; and (**c**) r_0.

The springback variability throughout the cup is mainly influenced by the uncertainty in the blank holder force, BHF, the anisotropy coefficient at 90° and the C parameter of Swift's law (Figure 12a). However, it can be noted that among these parameters, the parameter C of Swift's law is the most critical (Figure 12b), since it has a greater effect in areas where the springback variability reaches higher values. For springback, it is clear that the distributions of the Sobol and PAWN indices are different. This is to be expected as the springback distribution (see Figure 4) is bimodal and therefore a sensitivity analysis using Sobol indices is not appropriate in this case.

(a)

(b)

(c)

Figure 12. Distribution of PAWN (**left**) and Sobol (**right**) indices for springback: (**a**) BHF; (**b**) C; (**c**) r_{90}.

3.4. Maximum Sensitivity Indices per Region of the Square Cup

Figure 13 shows the input parameters for which the PAWN or Sobol indices are maximum in each zone of the square cup. For the equivalent plastic strain (Figure 13a), the geometry changes (Figure 13b), the thickness reduction (Figure 13c), the uncertainty in the anisotropy coefficient at 90° and the hardening coefficient were the most important in a large part of the cup; the uncertainty in the anisotropy coefficient at 0° also presented some areas of significant importance. The springback variability throughout the cup was significantly affected by the uncertainty in the blank holder force and the parameter C, with the uncertainty in the anisotropy coefficients at 45° and 90° also influential in certain locations of the cup (Figure 13d). As expected, the results for the PAWN and Sobol indices were identical for all output parameters except springback. The main difference was at the bottom and wall of the cup, where the PAWN indices indicate that the uncertainty in

the anisotropy coefficient at 45° is the most important parameter, while the Sobol indices consider the BHF to be the most important parameter.
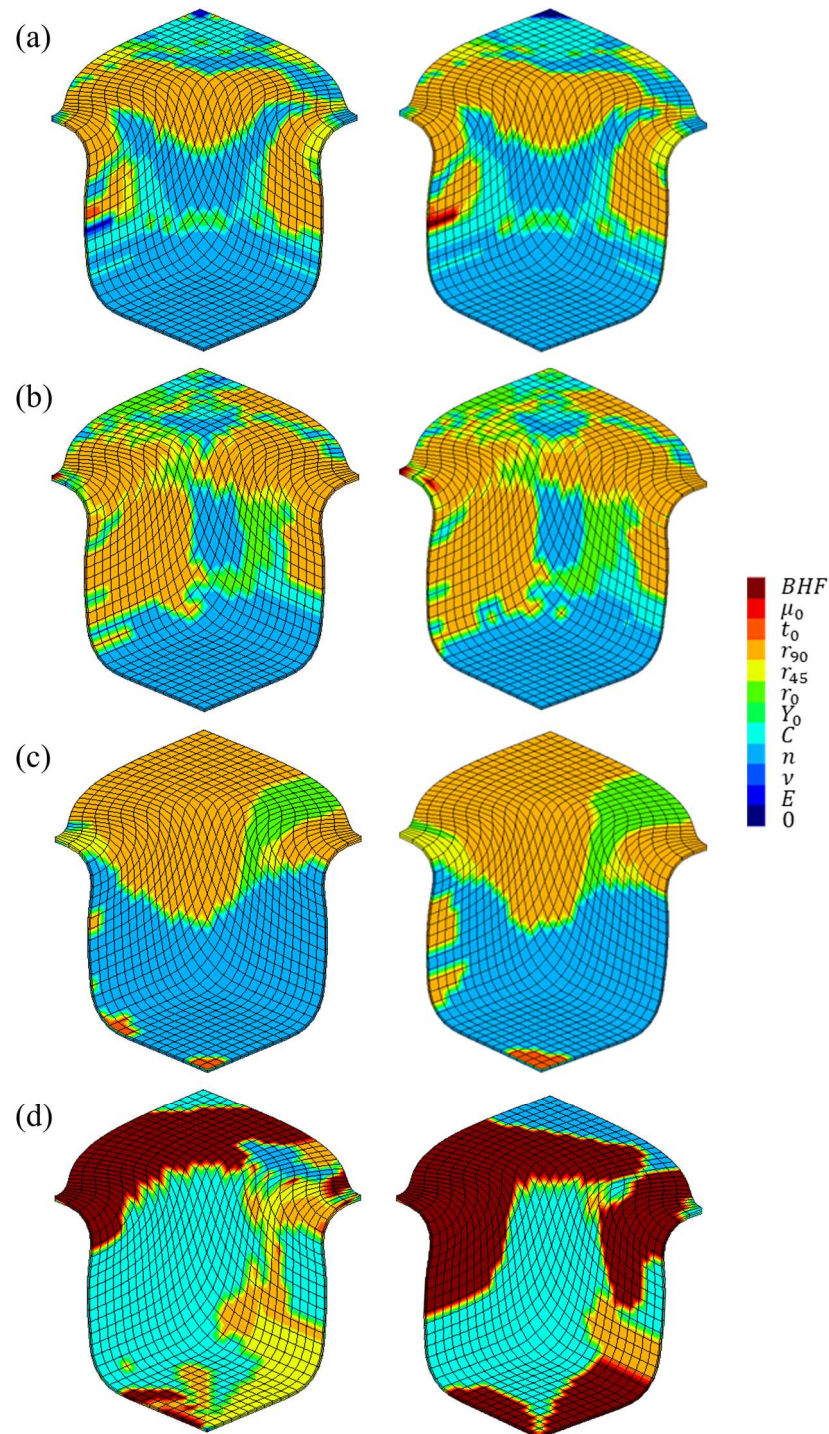

Figure 13. Parameters corresponding to the maximum PAWN index (**left**) and Sobol index (**right**) in each zone of for (**a**) EPS; (**b**) GC; (**c**) TR; and (**d**) SB.

3.5. Evolution of Sensitivity Indices for the Punch Force

Figure 14 shows the evolution of the PAWN and Sobol indices for the punch force as a function of its displacement. It can be seen that the influence of the uncertainty in the parameter C on the punch force variability increases with the punch displacement. The influence of the uncertainties in the hardening coefficient, n, and the yield stress, Y_0, on

the punch force variability increased initially but lost influence with the punch displacement. The uncertainty in the initial thickness has a constant influence on the punch force throughout its displacement. The primary distinction between the results obtained from the two-sensitivity analysis is the influence of the uncertainty in the anisotropy coefficient, r_0. However, the r_0 significant variations between 0 and 12 mm (for the Sobol indices) is artificial, i.e., it comes from errors in the calculation of Equation (12), when both variances in the dividend and divisor were approximately 0.
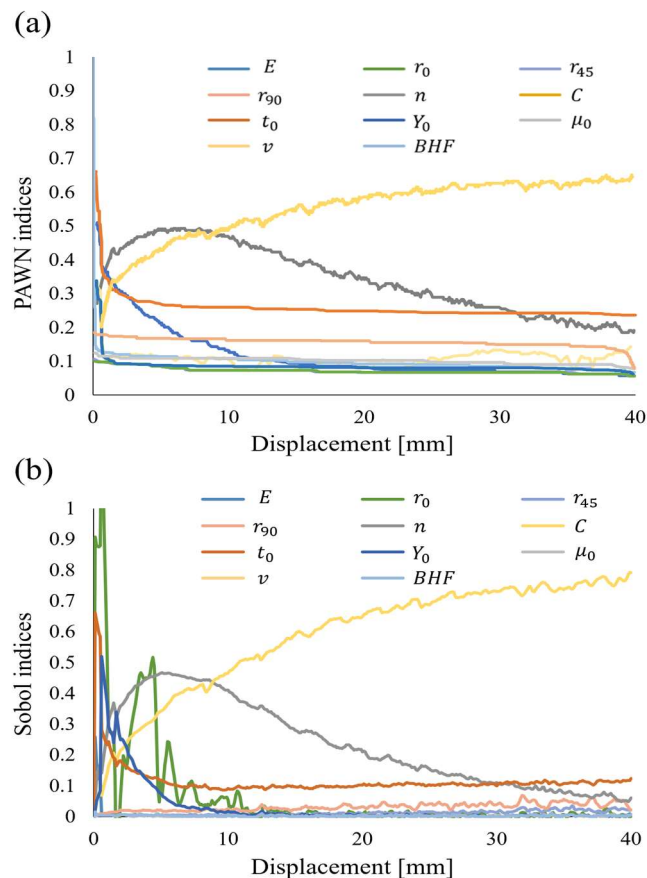
Figure 14. Indices of punch force as a function of displacement for (**a**) PAWN indices and (**b**) Sobol indices.

4. Conclusions

The main objective of this study was to quantify the influence of the uncertainty in material, friction, and process parameters on the forming results of a square cup. For this, a sensitivity analysis was carried out using two different techniques. It was concluded that the bottom of the cup is the area least affected by the uncertainty in the material, friction and process parameters. On the other hand, the flange, the radius of curvature of the die and the wall are the areas that show the greatest variability. For the equivalent plastic strain, the variability is more pronounced at the flange, as for geometry changes and springback. The uncertainty in the parameter C of Swift's law, the hardening coefficient and the initial sheet thickness significantly influence the variability of the punch force. The variability of equivalent plastic strain, thickness reduction and geometry changes are significantly influenced by the uncertainty in the hardening coefficient and the anisotropy coefficients. The variability of springback is significantly influenced by the uncertainty of parameter C of Swift's law, the hardening coefficient, the anisotropy coefficient at 90° and the blank holder force. It is worth noting that there is a difference between the results obtained using PAWN and Sobol indices, particularly in the case of the springback response. The study emphasizes that the type of distribution of the results plays a crucial role in the quality of the results, and it is therefore crucial to select the most appropriate sensitivity

analysis technique. For example, springback has a bimodal distribution, making PAWN indices more suitable for sensitivity analysis. The PAWN sensitivity analysis proved to be more computationally efficient than the Sobol sensitivity analysis, with improved accuracy for results following multimodal distributions. Although the PAWN indices are more efficient, evaluating them still requires a significant number of numerical simulations. To reduce the computational cost without compromising the quality of the results, we propose exploring the use of metamodelling techniques to evaluate both indices. This will allow to perform sensitivity analysis on more complex numerical models, that for instance consider deformable tools or the use of more advanced constitutive models that can describe texture evolution and the Bauschinger effect.

Author Contributions: Conceptualization, D.C.R. and A.F.G.P.; methodology, T.G.P., D.C.R. and A.F.G.P.; software, D.C.R. and A.F.G.P.; validation, T.G.P., D.C.R. and A.F.G.P.; formal analysis. D.C.R., T.G.P., M.C.O., A.F.G.P., P.A.P. and N.A.S.; writing—original draft preparation, T.G.P., D.C.R.; writing—review and editing, T.G.P., D.C.R., M.C.O., A.F.G.P., P.A.P. and N.A.S.; supervision, A.F.G.P.; project administration, A.F.G.P.; funding acquisition, A.F.G.P. All authors have read and agreed to the published version of the manuscript.

Data Availability Statement: The data presented in this study are available on request from the corresponding. The data are not publicly available due to privacy.

Conflicts of Interest: The authors declare no conflicts of interest.

References

1. Gronostajski, Z.; Pater, Z.; Madej, L.; Gontarz, A.; Lisiecki, L.; Łukaszek-Sołek, A.; Łuksza, J.; Mróz, S.; Muskalski, Z.; Muzykiewicz, W.; et al. Recent Development Trends in Metal Forming. *Arch. Civ. Mech. Eng.* **2019**, *19*, 898–941. [CrossRef]
2. de Souza, T.; Rolfe, B. Multivariate Modelling of Variability in Sheet Metal Forming. *J. Mater. Process. Technol.* **2008**, *203*, 1–12. [CrossRef]
3. Lim, Y.; Venugopal, R.; Ulsoy, A.G. Advances in the Control of Sheet Metal Forming. *IFAC Proc. Vol.* **2008**, *41*, 1875–1883. [CrossRef]
4. Hazra, S.; Williams, D.; Roy, R.; Aylmore, R.; Smith, A. Effect of Material and Process Variability on the Formability of Aluminium Alloys. *J. Mater. Process. Technol.* **2011**, *211*, 1516–1526. [CrossRef]
5. Han, S.S. The Influence of Tool Geometry on Friction Behavior in Sheet Metal Forming. *J. Mater. Process. Technol.* **1997**, *63*, 129–133. [CrossRef]
6. Majeske, K.D.; Hammett, P.C. Identifying Sources of Variation in Sheet Metal Stamping. *Int. J. Flex. Manuf. Syst.* **2003**, *15*, 5–18. [CrossRef]
7. Li, Y.Q.; Cui, Z.S.; Ruan, X.Y.; Zhang, D.J. Application of Six Sigma Robust Optimization in Sheet Metal Forming. In Proceedings of the 6th International Conference and Workshop on Numerical Simulation of 3D Sheet Metal Forming Process, Detroit, MI, USA, 15–19 August 2005; Volume 778 A, pp. 819–824.
8. Faes, M.; Van Doninck, B.; Imholz, M.; Moens, D. Product Reliability Optimization under Plate Sheet Forming Process Variability. In Proceedings of the 8th International Workshop on Reliable Computing, Liverpool, UK, 16–18 July 2018.
9. Ledoux, Y.; Sergent, A.; Arrieux, R. Impact of the Material Variability on the Stamping Process: Numerical and Analytical Analysis. In *AIP Conference Proceedings, Proceedings of the 9th International Conference on Numerical Methods in Industrial Forming Processes, Porto, Portugal, 17–21 June 2007*; AIP Publishing: New York, NY, USA, 2007; Volume 908, pp. 1213–1218.
10. Marretta, L.; Di Lorenzo, R. Influence of Material Properties Variability on Springback and Thinning in Sheet Stamping Processes: A Stochastic Analysis. *Int. J. Adv. Manuf. Technol.* **2010**, *51*, 117–134. [CrossRef]
11. Strano, M. A Technique for FEM Optimization under Reliability Constraint of Process Variables in Sheet Metal Forming. *Int. J. Mater. Form.* **2008**, *1*, 13–20. [CrossRef]
12. Huang, C.; Radi, B.; Hami, A. El Uncertainty Analysis of Deep Drawing Using Surrogate Model Based Probabilistic Method. *Int. J. Adv. Manuf. Technol.* **2016**, *86*, 3229–3240. [CrossRef]
13. Arnst, M.; Ponthot, J.P.; Boman, R. Comparison of Stochastic and Interval Methods for Uncertainty Quantification of Metal Forming Processes. *Comptes Rendus-Mec.* **2018**, *346*, 634–646. [CrossRef]

14. Shahi, V.J.; Masoumi, A.; Franciosa, P.; Ceglarek, D. Quality-Driven Optimization of Assembly Line Configuration for Multi-Station Assembly Systems with Compliant Non-Ideal Sheet Metal Parts. *Procedia CIRP* **2018**, *75*, 45–50. [CrossRef]

15. Dwivedy, M.; Kalluri, V. The Effect of Process Parameters on Forming Forces in Single Point Incremental Forming. *Procedia Manuf.* **2019**, *29*, 120–128. [CrossRef]

16. Prates, P.A.; Adaixo, A.S.; Oliveira, M.C.; Fernandes, J.V. Numerical Study on the Effect of Mechanical Properties Variability in Sheet Metal Forming Processes. *Int. J. Adv. Manuf. Technol.* **2018**, *96*, 561–580. [CrossRef]

17. Marques, A.E.; Prates, P.A.; Pereira, A.F.G.; Oliveira, M.C.; Fernandes, J.V.; Ribeiro, B.M. Performance Comparison of Parametric and Non-Parametric Regression Models for Uncertainty Analysis of Sheet Metal Forming Processes. *Metals* **2020**, *10*, 457. [CrossRef]

18. Dib, M.A.; Oliveira, N.J.; Marques, A.E.; Oliveira, M.C.; Fernandes, J.V.; Ribeiro, B.M.; Prates, P.A. Single and Ensemble Classifiers for Defect Prediction in Sheet Metal Forming under Variability. *Neural Comput. Appl.* **2020**, *32*, 12335–12349. [CrossRef]

19. Bérend, N.; Le Riche, R. Comparison of Different Global Sensitivity Analysis Methods for Aerospace Vehicle Optimal Design. In Proceedings of the 10th World Congress on Structural and Multidisciplinary Optimization, Orlando, FL, USA, 19–24 May 2013.

20. Pianosi, F.; Wagener, T. A Simple and Efficient Method for Global Sensitivity Analysis Based On cumulative Distribution Functions. *Environ. Model. Softw.* **2015**, *67*, 1–11. [CrossRef]

21. Pianosi, F.; Wagener, T. Distribution-Based Sensitivity Analysis from a Generic Input-Output Sample. *Environ. Model. Softw.* **2018**, *108*, 197–207. [CrossRef]

22. Puy, A.; Lo Piano, S.; Saltelli, A. A Sensitivity Analysis of the PAWN Sensitivity Index. *Environ. Model. Softw.* **2020**, *127*, 104679. [CrossRef]

23. Pereira, A.F.G.; Ruivo, M.F.; Oliveira, M.C.; Fernandes, J.V.; Prates, P.A. Numerical Study of the Square Cup Stamping Process: A Stochastic Analysis. In Proceedings of the ESAFORM 2021—24th International Conference on Material Forming, Liege, Belgium, 16–14 April 2021; PoPuPS (University of Liege Library): Liège, Belgium, 2021.

24. Bayraktar, E.; Altintaş, S. Square Cup Deep Drawing Experiments. In Proceedings of the 2nd International Conference Numerical Simulation of 3-D Sheet Metal Forming Processes, NUMISHEET '93, Isehara, Japan, 31 August–2 September 1993; p. 441.

25. Neto, D.M.; Oliveira, M.C.; Menezes, L.F. Surface Smoothing Procedures in Computational Contact Mechanics. *Arch. Comput. Methods Eng.* **2017**, *24*, 37–87. [CrossRef]

26. Menezes, L.F.; Teodosiu, C. Three-Dimensional Numerical Simulation of the Deep-Drawing Process Using Solid Finite Elements. *J. Mater. Process. Technol.* **2000**, *97*, 100–106. [CrossRef]

27. Hill, R. A Theory of the Yielding and Plastic Flow of Anisotropic Metals. *Proc. R. Soc. London Ser. A Math. Phys. Sci.* **1948**, *193*, 281–297.

28. Swift, H.W. Plastic Instability under Plane Stress. *J. Mech. Phys. Solids* **1952**, *1*, 1–18. [CrossRef]

29. Sobol', I.M. On the Distribution of Points in a Cube and the Approximate Evaluation of Integrals. *USSR Comput. Math. Math. Phys.* **1967**, *7*, 86–112. [CrossRef]

30. Saltelli, A.; Ratto, M.; Andres, T.; Campolongo, F.; Cariboni, J.; Gatelli, D.; Saisana, M.; Tarantola, S. *Global Sensitivity Analysis. The Primer*; John Wiley & Sons: Hoboken, NJ, USA, 2008. [CrossRef]